
This manuscript has been submitted for publication in Nature Communications. Please note that this is a preprint which has undergone one round of peer review but has not yet been formally accepted for publication. Subsequent versions may have slightly different content. If accepted, the final version of this manuscript will be available via the ‘Peer-reviewed Publication DOI’ link on the right-hand side of this webpage. Please feel free to contact any of the authors; we welcome the feedback.

1 **Fault rock heterogeneity produces fault weakness and promotes unstable slip**

2

3 John D. Bedford^{1*}, Daniel R. Faulkner¹ & Nadia Lapusta^{2,3}

4 ¹*Rock Deformation Laboratory, Department of Earth, Ocean and Ecological Sciences, University of*
5 *Liverpool*

6 ²*Department of Mechanical and Civil Engineering, Division of Engineering and Applied Science,*
7 *California Institute of Technology*

8 ³*Seismological Laboratory, Division of Geological and Planetary Sciences, California Institute of*
9 *Technology*

10 *Corresponding author: jbedford@liverpool.ac.uk

11

12 **Abstract**

13 Geological heterogeneity is abundant in crustal fault zones; however, its role in controlling the
14 mechanical behaviour of faults is poorly constrained. Here, we present laboratory friction experiments
15 on laterally heterogeneous faults, with patches of strong, rate-weakening quartz gouge and weak, rate-
16 strengthening clay gouge. The experiments show that the heterogeneity leads to a significant strength
17 reduction and decrease in frictional stability in comparison to compositionally identical faults with
18 homogeneously mixed gouges typically used in the lab. We identify a combination of weakening
19 effects, including smearing of the weak clay; differential compaction of the two gouges redistributing
20 normal stress; and shear localization producing stress concentrations in the strong quartz patches. The
21 results demonstrate that small-scale geological heterogeneity has pronounced effects on fault strength
22 and stability, and by extension on the occurrence of slow-slip transients versus earthquake ruptures and
23 the characteristics of the resulting events, and should be incorporated in lab experiments, fault friction
24 laws, and earthquake source modelling.

25

26 Introduction

27 Many large crustal faults have been shown to be frictionally weak¹⁻⁶ when compared to
28 laboratory measurements of quasi-static fault friction. The coefficient of friction $\mu = \tau/\bar{\sigma}_n$, where μ is
29 the shear stress during slip and $\bar{\sigma}_n$ is the effective normal stress, of most geological materials is typically
30 measured in the laboratory to be between 0.6-0.85 at slow slip speeds, independent of rock type⁷, with
31 the exception of a few weak minerals, predominantly phyllosilicates^{7,8}. Possible explanations for weak
32 faults in nature, where the apparent μ at which faults operate is often less than 0.5, include localization
33 of weak minerals along structural foliations⁹⁻¹², dynamic weakening during seismic slip¹³, and elevated
34 pore fluid pressure interpreted as lower friction coefficients^{14,15}. As well as being apparently weak,
35 many crustal faults also exhibit a spectrum of slip behaviour, with earthquake slip and aseismic creep
36 often occurring on the same fault^{16,17} and slow slip phenomena being prevalent at all crustal depths¹⁸.
37 While the apparent weakness of faults and spectrum of slip behaviour can be attributed to the effects of
38 spatially varying and temporally evolving confinement, temperature, and pore fluid pressure, it is clear
39 that heterogeneity in fault-zone rocks (Fig. 1a) can also play an important^{19,20}, if not dominant, role.

40 Geological investigations have shown that heterogeneity in fault-zone rocks occurs over many
41 different scales, from submillimetre-scale structural foliations^{9,10}, centimetre- to meter-scale blocks
42 within a shear zone *mélange*²¹, hundreds-of-meters scale where lenses of damaged protolith can be
43 entrapped within the core of wide (km-scale) fault zones^{22,23} (e.g. Fig. 1a), to tens-of-kilometers scale
44 variations in rock types^{10,24}. The role of large-scale fault rock heterogeneity has been highlighted in a
45 number of studies; for example, it has been suggested that heterogeneities such as seamounts can act as
46 earthquake nucleation sites and control the seismogenic behaviour of subduction-zone megathrust
47 faults^{25,26}. However, the importance of small-scale fault rock heterogeneity in controlling fault slip
48 behaviour, average fault strength, and fault stability is still uncertain.

49 Here, the effect of fault rock heterogeneity on fault strength and slip behaviour is investigated
50 by a series of laboratory friction experiments on simulated laterally heterogeneous faults. The faults
51 consist of different sized patches of strong, rate-weakening quartz, and weak, rate-strengthening clay
52 fault gouges. Until now, the majority of experimental investigations have been performed using

53 mixtures of different fault gouge materials with varying frictional properties, where the materials are
54 homogeneously mixed together^{27–30}; intact wafers of natural gouge have also been used^{9,10}. In this work,
55 experiments are performed on both homogeneously mixed and spatially heterogeneous gouge layers
56 consisting of quartz, frictionally strong and rate-weakening, and kaolinite clay powder, frictionally
57 weak and rate-strengthening. The fault gouge layers (50 mm long, 20 mm wide, with an initial thickness
58 of 1 mm) are sheared in a direct shear arrangement (Fig. 1b, see also Supplementary Fig. 1) within a
59 triaxial deformation apparatus (see Methods). The heterogeneous gouge layers are constructed by
60 placing different sized patches of fine-grained quartz and clay powder (both <5 μm grain size) adjacent
61 to each other in a symmetrical pattern, with a central quartz patch being bound by two clay patches (Fig.
62 1b). This symmetrical arrangement ensures that no misalignment between the direct shear forcing
63 blocks would occur as a result of any differential compaction between the different materials;
64 furthermore, the amount of gouge material used (measured by weight prior to the experiment) was
65 calculated so that the thickness of the quartz and clay gouges were the same after initial pressurization
66 and a small amount of shear (Supplementary Fig. 2). The normal stress is applied by the confining
67 pressure (P_c) in the triaxial apparatus, held constant at 60 MPa for all tests in this study, and the pore
68 fluid pressure (P_f) within the gouge is servo-controlled at a constant value of 20 MPa, resulting in the
69 effective normal stress $\bar{\sigma}_n = 40$ MPa ($\bar{\sigma}_n = P_c - P_f$). The gouge layers are sheared up to a maximum
70 displacement of 8.5 mm (shear strain ≈ 10 , given the final layer thickness of ~ 0.85 mm). Monitoring
71 the evolution of shear stress while applying velocity steps from 0.3 to 3 $\mu\text{m}\cdot\text{s}^{-1}$ and back allows the
72 experiments to quantify the rate-and-state friction parameters that determine the stability of fault slip³¹.
73 These sliding velocities are sufficiently slow, given the gouge permeability, to ensure that pore pressure
74 transients do not build up within the gouge layer during shearing³². The sizes of the strong yet unstable
75 quartz and weak but stable clay patches are varied to investigate the role of different scales of
76 heterogeneity on the magnitude and stability of fault friction.

77 **Results**

78 The experimental results indicate pronounced differences between the behaviour of laterally
79 heterogeneous faults compared to the laterally homogeneous faults with mixed gouge (Figure 1). All

80 experiments are characterized by an initially rapid increase in shear stress during the loading phase,
81 before the samples clearly yield - i.e., shear inelastically - after approximately 1 mm of displacement.
82 After that, the friction coefficient μ of the homogeneously mixed gouge layers remains relatively
83 constant (Fig. 1d), with rate-and-state effects consistent with results from previous experimental
84 studies²⁸⁻³⁰. In contrast, the heterogeneous gouge layers all show ubiquitous weakening (Fig. 1c), with
85 μ evolving towards the value of the weaker clay phase. To ensure that the observed weakening was not
86 caused by the arrangement of the different gouge patches in the experiments, tests were performed
87 where the symmetry of the heterogeneous layers was reversed (i.e., a central clay patch bound by two
88 quartz patches). These tests also exhibit similar weakening (Supplementary Fig. 3) suggesting that it is
89 the heterogeneity itself, not the arrangement of the different materials, that causes the weakening. Stable
90 sliding is observed for all homogeneously mixed faults and the majority of heterogeneous faults.
91 However, when the quartz patch in the heterogeneous layers comprises $\geq 80\%$ of the total sliding area,
92 unstable stick-slip sliding emerges, typically triggered by up-steps in the sliding velocity (Fig. 1c).

93 The observed weakening of the heterogeneous faults is greater than can be explained by the
94 observed smearing of the clay patches. Microstructural analysis of a heterogeneous layer recovered at
95 the end of an experiment (Fig. 2a) shows smearing of clay into localized boundary Y-shears that
96 propagate into the quartz patch. With progressive smearing and localization of the clay phase (Fig. 2b),
97 the strength of the layer overall is expected to decrease as a greater proportion of the slipping surface
98 can be located within the weak clay phase. As the frictional strength of the endmember gouge
99 compositions is known (i.e. 100% quartz and 100% clay in Fig. 1c), the predicted weakening due to
100 smearing can be calculated (Fig. 2c) by assuming that the overall strength is determined by the strength
101 of the two gouges acting in series, based on their relative proportions (the arithmetic mean of μ , based
102 on the proportions of clay and quartz within the layer). The predicted weakening, associated with the
103 relative increase of the clay patches is considerably less than the observed weakening in the experiments
104 (Fig. 2c), suggesting that clay smearing alone is not responsible for the progressive weakening of
105 heterogeneous faults.

106 The velocity steps from Figure 1c-d are used to calculate the evolution in the rate-and-state
107 friction parameter ($a - b$), which determines the frictional stability of the fault^{33,34}. When $a - b > 0$, the
108 sliding behaviour is rate-strengthening, suppressing instabilities and promoting stable sliding, whereas
109 when $a - b < 0$, the sliding behaviour is rate-weakening which promotes unstable slip behaviour and
110 the occurrence of stick-slips in the laboratory. The values of ($a - b$) are consistently lower (i.e., less
111 rate-strengthening) in the heterogeneous faults throughout the experiment (Figure 3a-c). This finding
112 indicates that the heterogeneous faults are closer to the potentially unstable, rate-weakening regime than
113 their homogeneous counterparts.

114 For the homogeneous faults with the pure quartz gouge and the heterogeneous faults where the
115 quartz patch comprises $\geq 80\%$ of the total sliding area, only the first velocity step can be used to
116 determine the rate dependence due to the occurrence of stick-slip instabilities triggered by subsequent
117 velocity steps. However, this initial velocity step at 1.5 mm displacement does show negative values of
118 ($a - b$) associated with rate-weakening behaviour (Fig. 3a), which is consistent with the occurrence of
119 stick-slip instabilities later in the experiment. All of the calculated rate-and state friction data are
120 presented in Supplementary Table 1.

121 Discussion

122 Our experiments show that laterally heterogeneous fault gouge layers weaken significantly in
123 comparison to homogeneous layers, pointing to heterogeneity-induced weakening effects. We
124 hypothesize that the weakening occurs due to a combination of mechanisms, all of which can affect
125 natural faults. The mechanical smearing of the weak phase with slip can reduce the overall shear
126 resistance as shear is likely to localize within the weak phase, although this mechanism by itself can
127 explain only part of the observed weakening (Fig. 2c). Another contributing mechanism can be
128 differential compaction of the weak and strong phases during shear (Supplementary Fig. 2) which would
129 result in a redistribution of normal stress along the shearing layer, with the weaker phase supporting
130 higher normal stresses (see Supplementary Information for further discussion of this effect). The
131 differential compaction can produce significant weakening effects but it is poorly constrained, with the
132 conclusions based on end-member tests of pure quartz and clay samples under constant normal stress,

133 highlighting the need to better capture and characterize the compaction/dilation effects in gouge
134 experiments. Finally, additional weakening can be due to shear occurring in the weaker clay gouge that
135 produces stress concentrations along localized Y-shear bands that propagate through the stronger quartz
136 patches leading to enhanced weakening. Similar shear stress concentrations have also been suggested
137 to promote slip events in strong, rate-weakening gouge patches in recent low normal stress experiments
138 on decimeter-scale heterogeneous faults³⁵.

139 Competency contrasts between strong and weak materials in shear zone mélanges have been
140 suggested previously to be important in controlling the average fault strength and rheology³⁶, with only
141 a small amount of well-connected weak material needed to reduce fault strength when structural
142 foliations are well developed⁹. Here we show that the average frictional strength of laterally
143 heterogeneous faults is not just an average of the respective friction properties, and that competency
144 contrasts can substantially reduce the fault strength, even when structural foliations are in their infancy
145 and unconnected (Fig. 2a).

146 Contrasting material properties within fault zones have also been suggested to give rise to
147 mixed fault slip behaviour³⁷ and exert an important control on earthquake rupture dynamics^{38,39}.
148 Heterogeneities are also thought to strongly influence the sliding behaviour of other types of frictional
149 interface, such as at the base of glaciers⁴⁰. Our experiments show that heterogeneity has an overall
150 destabilizing effect when compared to homogeneous faults (Fig. 3). In the heterogeneous experiments,
151 the patch size of the strong rate-weakening material ultimately determines whether stable or unstable
152 slip occurs (Fig. 1c). When the strong patch comprises <80% of the fault length, the fault slides in a
153 stable aseismic fashion. However, when the strong patch comprises $\geq 80\%$ of the layer, stick-slip
154 instabilities occur. As shown previously in experimental studies on rate-weakening quartz gouges,
155 microstructural evolution and deformation localization into discrete shear bands is a prerequisite for
156 unstable stick-slip behaviour^{41,42}. Therefore, in a heterogeneous fault, the slip behaviour would be
157 dictated by the competing processes of fault stabilization via deformation in weak rate-strengthening
158 materials, versus destabilization caused by localization within the strong rate-weakening patches. When

159 the strong rate-weakening patches are large enough for their internal structure to evolve independently,
160 earthquake nucleation may occur.

161 The role of heterogeneity is summarized in Figure 4, where, for a given clay-quartz mixture,
162 heterogeneous faults are weaker and more unstable relative to their homogeneous equivalents. Although
163 it is often invoked that large-scale heterogeneities are responsible for the spectrum of slip behaviour
164 observed on natural faults^{16,17}, the results presented here highlight the potential of small-scale
165 heterogeneities, which are also abundant in natural fault zones^{9,10,21}, to exert a significant control on
166 fault zone strength and stability.

167 To summarize, we show that, by introducing a simple heterogeneous structure into a fault zone,
168 the fault strength is substantially reduced and the stability of the experimental fault is overall decreased
169 in comparison to compositionally identical but homogeneously mixed gouges. Our data, along with the
170 abundance and complexity of heterogeneity that occurs over many different scales in nature^{9,10,21-24},
171 suggest that interactions between heterogeneously distributed materials with different frictional
172 properties likely exerts an important control over the mechanical strength and influences whether
173 tectonic faults experience aseismic or earthquake slip. The smaller the scale of heterogeneity, the more
174 likely it is to be intractable in modelling earthquake source processes and hence ignored. This
175 consideration, together with our findings, necessitates further laboratory experiments on heterogeneous
176 faults and inclusion of the small-scale heterogeneity effects into larger-scale constitutive laws for
177 modelling fault processes of societal interest, such as nucleation of natural and induced earthquakes.

178

179 **Methods**

180 *Experimental Procedure*

181 The gouge layers are deformed in a direct-shear arrangement (Supplementary Fig. 1) within a
182 triaxial deformation apparatus⁴³. The layers (1 mm initial thickness), prepared in either heterogeneous
183 patches or as a homogeneous quartz-clay mixture, are placed between the direct-shear forcing blocks
184 and soft silicone spacers are positioned at each end so that displacement can be accommodated without

185 supporting any load (Supplementary Fig. 1). Once the gouge layer is constructed, the direct-shear
186 arrangement is surrounded by a low-friction polytetrafluoroethylene (PTFE) sleeve (0.25 mm thickness)
187 to minimize jacket friction in the vicinity of the layer, before being placed into a 3 mm thick PVC jacket.
188 The jacketed direct-shear arrangement is then placed in between the platens of the sample assembly
189 which is inserted into the pressure vessel of the triaxial apparatus. In this geometry, the normal stress
190 (σ_n) is applied to the gouge layer by the confining pressure. The pore-fluid pressure is introduced to
191 the layer through three porous disks, embedded in each direct-shear forcing block, which are positioned
192 to ensure an even distribution of pore fluid throughout the layer. Deionized water is used as the pore
193 fluid. Both the confining and pore-fluid pressures are held constant throughout the experiments by
194 servo-controlled pumps on each pressure system, with a resolution better than 0.01 MPa. The layers are
195 sheared by the axial piston of the triaxial apparatus and velocity steps are imposed to calculate the rate-
196 and-state friction parameters. The evolution of shear stress is monitored by an internal force gauge
197 within the axial piston, with a measurement resolution of better than 0.05 kN.

198

199 **Data Availability**

200 The associated experimental data files for this research can be accessed in National Geoscience Data
201 Center (NGDC) via the following link:

202 <https://webapps.bgs.ac.uk/services/ngdc/accessions/index.html#item164865>

203

204 **References**

- 205 1. Lachenbruch, A. H. & Sass, J. H. Heat flow and energetics of the San Andreas Fault Zone. *J.*
206 *Geophys. Res.* **85**, 6185–6222 (1980).
- 207 2. Zoback, M. D. *et al.* New Evidence on the state of stress of the San Andreas fault system.
208 *Science* **238**, 1105–1111 (1987).
- 209 3. Copley, A., Avouac, J.-P., Hollingsworth, J. & Leprince, S. The 2001 Mw 7.6 Bhuj

- 210 earthquake, low fault friction, and the crustal support of plate driving forces in India. *J.*
211 *Geophys. Res.* **116**, (2011).
- 212 4. Lamb, S. Shear stresses on megathrusts: Implications for mountain building behind subduction
213 zones. *J. Geophys. Res.* **111**, (2006).
- 214 5. Holdsworth, R. E. Weak Faults — Rotten Cores. *Science* **303**, 181–182 (2004).
- 215 6. Chiaraluze, L., Chiarabba, C., Collettini, C., Piccinini, D. & Cocco, M. Architecture and
216 mechanics of an active low-angle normal fault: Alto Tiberina Fault, northern Apennines, Italy.
217 *J. Geophys. Res.* **112**, (2007).
- 218 7. Byerlee, J. Friction of Rocks. *Pure Appl. Geophys.* **116**, 615–626 (1978).
- 219 8. Ikari, M. J., Marone, C. & Saffer, D. M. On the relation between fault strength and frictional
220 stability. *Geology* **39**, 83–86 (2011).
- 221 9. Collettini, C., Niemeijer, A., Viti, C. & Marone, C. Fault zone fabric and fault weakness.
222 *Nature* **462**, 907–911 (2009).
- 223 10. Tesei, T., Collettini, C., Barchi, M. R., Carpenter, B. M. & Di Stefano, G. Heterogeneous
224 strength and fault zone complexity of carbonate-bearing thrusts with possible implications for
225 seismicity. *Earth Planet. Sci. Lett.* **408**, 307–318 (2014).
- 226 11. Carpenter, B. M., Marone, C. & Saffer, D. M. Weakness of the San Andreas Fault revealed by
227 samples from the active fault zone. *Nat. Geosci.* **4**, 251–254 (2011).
- 228 12. Attanayake, J. *et al.* Rupture characteristics and bedrock structural control of the 2016 Mw 6.0
229 intraplate earthquake in the Petermann Ranges, Australia. *Bull. Seismol. Soc. Am.* **110**, 1037–
230 1045 (2020).
- 231 13. Di Toro, G. *et al.* Fault lubrication during earthquakes. *Nature* **471**, 494–498 (2011).
- 232 14. Rice, J. R. Fault stress states, pore pressure distributions, and the weakness of the San Andreas
233 Fault. in *Fault Mechanics and Transport Properties of Rocks* (eds. Evans, B. & Wong, T.) vol.

- 234 51 475–503 (Academic Press, 1992).
- 235 15. Faulkner, D. R. & Rutter, E. H. Can the maintenance of overpressured fluids in large strike-
236 slip fault zones explain their apparent weakness? *Geology* **29**, 503–506 (2001).
- 237 16. Avouac, J.-P. From geodetic imaging of seismic and aseismic fault slip to dynamic modeling
238 of the seismic cycle. *Annu. Rev. Earth Planet. Sci.* **43**, 233–271 (2015).
- 239 17. Thomas, M. Y., Avouac, J.-P., Champenois, J., Lee, J.-C. & Kuo, L.-C. Spatiotemporal
240 evolution of seismic and aseismic slip on the Longitudinal Valley Fault, Taiwan. *J. Geophys.*
241 *Res. Solid Earth* **119**, 5114–5139 (2014).
- 242 18. Bürgmann, R. The geophysics, geology and mechanics of slow fault slip. *Earth Planet. Sci.*
243 *Lett.* **495**, 112–134 (2018).
- 244 19. Collettini, C., Tesei, T., Scuderi, M. M., Carpenter, B. M. & Viti, C. Beyond Byerlee friction,
245 weak faults and implications for slip behavior. *Earth Planet. Sci. Lett.* **519**, 245–263 (2019).
- 246 20. Barnes, P. M. *et al.* Slow slip source characterized by lithological and geometric heterogeneity.
247 *Sci. Adv.* **6**, (2020).
- 248 21. Fagereng, Å. Frequency-size distribution of competent lenses in a block-in-matrix mélange:
249 Imposed length scales of brittle deformation? *J. Geophys. Res.* **116**, (2011).
- 250 22. Faulkner, D. R., Lewis, A. C. & Rutter, E. H. On the internal structure and mechanics of large
251 strike-slip fault zones: field observations of the Carboneras fault in southeastern Spain.
252 *Tectonophysics* **367**, 235–251 (2003).
- 253 23. Faulkner, D. R. *et al.* A review of recent developments concerning the structure, mechanics
254 and fluid flow properties of fault zones. *J. Struct. Geol.* **32**, 1557–1575 (2010).
- 255 24. Rutter, E. H., Faulkner, D. R. & Burgess, R. Structure and geological history of the Carboneras
256 Fault Zone, SE Spain: Part of a stretching transform fault system. *J. Struct. Geol.* **45**, 68–86
257 (2012).

- 258 25. Bilek, S. L. & Lay, T. Tsunami earthquakes possibly widespread manifestations of frictional
259 conditional stability. *Geophys. Res. Lett.* **29**, 1673 (2002).
- 260 26. Kirkpatrick, J. D. *et al.* Subduction megathrust heterogeneity characterized from 3D seismic
261 data. *Nat. Geosci.* **13**, 369–374 (2020).
- 262 27. Crawford, B. R., Faulkner, D. R. & Rutter, E. H. Strength, porosity, and permeability
263 development during hydrostatic and shear loading of synthetic quartz-clay fault gouge. *J.*
264 *Geophys. Res.* **113**, (2008).
- 265 28. Tembe, S., Lockner, D. A. & Wong, T.-F. Effect of clay content and mineralogy on frictional
266 sliding behavior of simulated gouges: Binary and ternary mixtures of quartz, illite, and
267 montmorillonite. *J. Geophys. Res.* **115**, (2010).
- 268 29. Takahashi, M., Mizoguchi, K., Kitamura, K. & Masuda, K. Effects of clay content on the
269 frictional strength and fluid transport property of faults. *J. Geophys. Res.* **112**, (2007).
- 270 30. Kenigsberg, A. R., Rivière, J., Marone, C. & Saffer, D. M. Evolution of elastic and mechanical
271 properties during fault shear: The roles of clay content, fabric development, and porosity. *J.*
272 *Geophys. Res. Solid Earth* **125**, (2020).
- 273 31. Skarbek, R. M. & Savage, H. M. RSFit3000 : A MATLAB GUI-based program for
274 determining rate and state frictional parameters from experimental data. *Geosphere* **15**, 1665–
275 1676 (2019).
- 276 32. Faulkner, D. R., Sanchez-Roa, C., Boulton, C. & den Hartog, S. A. M. Pore fluid pressure
277 development in compacting fault gouge in theory, experiments, and nature. *J. Geophys. Res.*
278 *Solid Earth* **123**, 226–241 (2018).
- 279 33. Scholz, C. H. Earthquakes and friction laws. *Nature* **391**, 37–42 (1998).
- 280 34. Marone, C. Laboratory-derived friction laws and their application to seismic faulting. *Annu.*
281 *Rev. Earth Planet. Sci.* **26**, 643–696 (1998).

- 282 35. Buijze, L., Guo, Y., Niemeijer, A. R., Ma, S. & Spiers, C. J. Effects of heterogeneous gouge
283 segments on the slip behavior of experimental faults at dm scale. *Earth Planet. Sci. Lett.* **554**,
284 116652 (2021).
- 285 36. Fagereng, Å. & Sibson, R. H. Mélange rheology and seismic style. *Geology* **38**, 751–754
286 (2010).
- 287 37. Skarbek, R. M., Rempel, A. W. & Schmidt, D. A. Geologic heterogeneity can produce
288 aseismic slip transients. *Geophys. Res. Lett.* **39**, (2012).
- 289 38. Noda, H. & Lapusta, N. Stable creeping fault segments can become destructive as a result of
290 dynamic weakening. *Nature* **493**, 518–521 (2013).
- 291 39. Bayart, E., Svetlizky, I. & Fineberg, J. Rupture dynamics of heterogeneous frictional
292 interfaces. *J. Geophys. Res. Solid Earth* **123**, 3828–3848 (2018).
- 293 40. Bahr, D. B. & Rundle, J. B. Stick-slip statistical mechanics at the bed of a glacier. *Geophys.*
294 *Res. Lett.* **23**, 2073–2076 (1996).
- 295 41. Scuderi, M. M., Collettini, C., Viti, C., Tinti, E. & Marone, C. Evolution of shear fabric in
296 granular fault gouge from stable sliding to stick slip and implications for fault slip mode.
297 *Geology* **45**, 731–734 (2017).
- 298 42. Bedford, J. D. & Faulkner, D. R. The role of grain size and effective normal stress on
299 localization and the frictional stability of simulated quartz gouge. *Geophys. Res. Lett.* **48**,
300 e2020GL092023 (2021).
- 301 43. Faulkner, D. R. & Armitage, P. J. The effect of tectonic environment on permeability
302 development around faults and in the brittle crust. *Earth Planet. Sci. Lett.* **375**, 71–77 (2013).
- 303

304 **Acknowledgements**

305 Gary Coughlan is thanked for assistance in developing and maintaining the experimental apparatus.
306 We are grateful to Elisabetta Mariani for help with and maintenance of the SEM facilities. This work
307 is supported by Natural Environment Research Council grant NE/P002943/1.

308

309 **Author contributions**

310 J.D.B and D.R.F developed the main ideas. J.D.B performed the experiments, ran microstructural
311 analyses and produced the initial manuscript. All authors contributed to interpreting the results and
312 editing the manuscript.

313

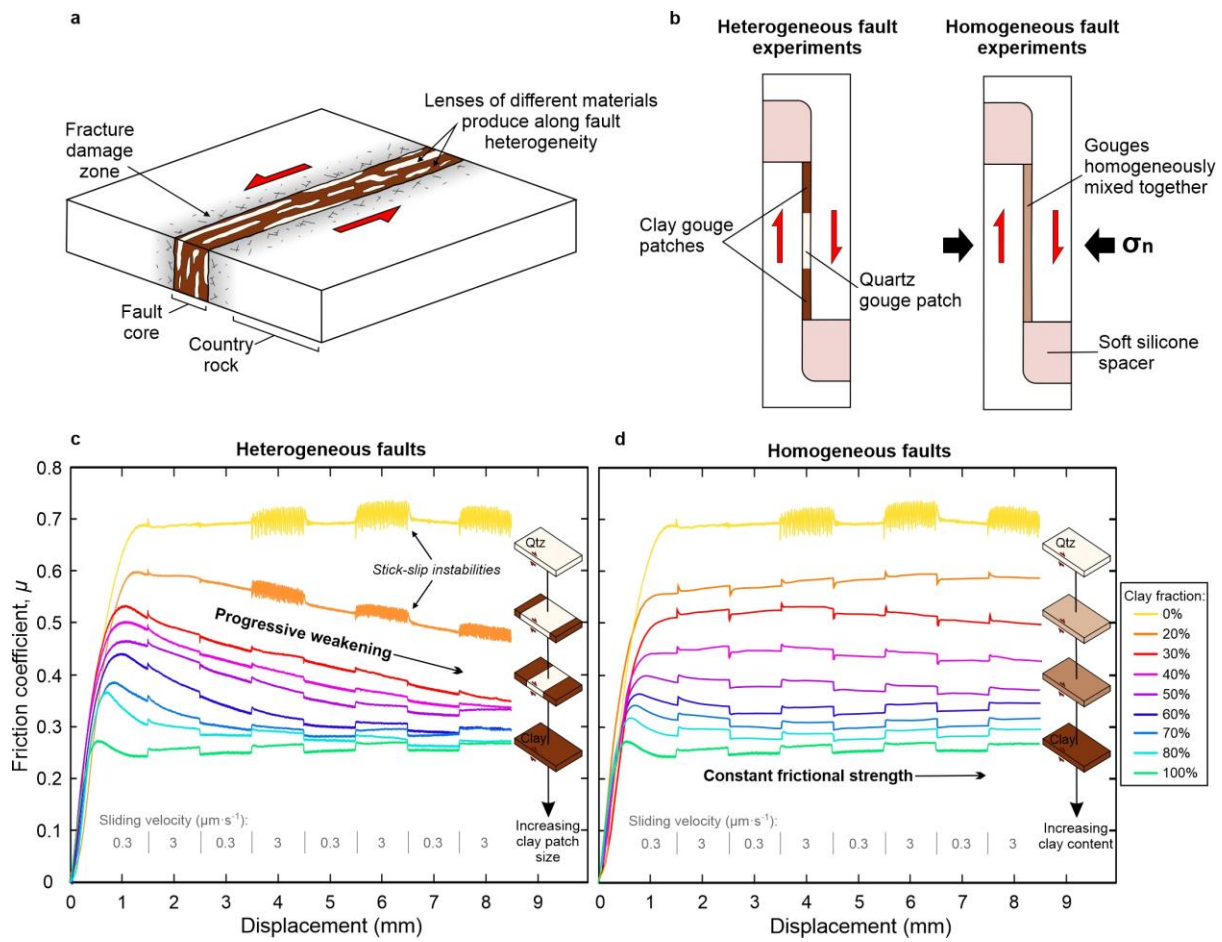
314 **Competing interests**

315 The authors declare no competing interests.

316

317 **Materials and correspondence**

318 Correspondence and material requests should be addressed to J.D.B.



319

320 **Figure 1| Mechanical behaviour of laterally heterogeneous vs. homogeneously mixed clay-quartz**

321 **fault gouge layers. a,** Schematic diagram of a typical natural fault zone showing how lenses of different

322 materials trapped within the fault core produces a heterogeneous structure. **b,** Simplified diagrams of

323 the experimental setup for the heterogenous fault experiments, where quartz and clay gouges are

324 separated into adjacent patches, and homogenous fault experiments where the two gouges are

325 homogeneously mixed together. **c,** Evolution of the friction coefficient (μ) with displacement for the

326 heterogeneous experimental faults and, **d,** the homogeneous experimental faults. Heterogeneous faults

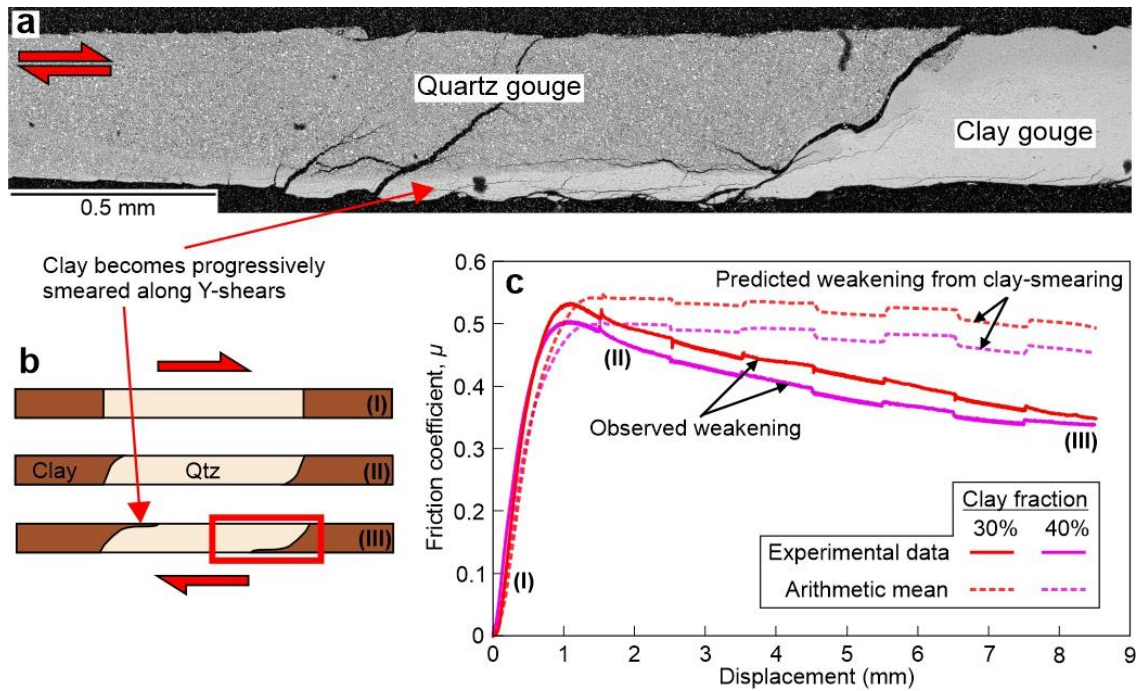
327 show ubiquitous post-yield weakening with increasing displacement, in contrast to homogeneous faults

328 where μ remains relatively constant once the layer has yielded after approximately 1 mm of slip. For

329 pure quartz and heterogeneous faults where the quartz patch comprises $\geq 80\%$ of the total fault area,

330 stick-slip instabilities occur, triggered by up-steps in the sliding velocity.

331



332

333 **Figure 2| Microstructural evolution and predicted weakening of the heterogeneous fault gouge**

334 **layers due to smearing of clay. a,** Backscatter electron image of the interface between a clay-quartz

335 patch recovered at the end of an experiment. The clay phase becomes smeared along a boundary Y-

336 shear plane that propagates into the quartz patch. Since it is difficult to keep the gouge layer intact upon

337 removal from the direct shear assembly at the end of the experiment, the full extent of the localized

338 shear band was not recovered. **b,** Schematic diagram showing the evolution of the fault gouge layers

339 with progressive smearing of the clay phase along localized Y-boundary shears (red box shows the

340 location of the micrograph in **a**). **c,** Observed weakening versus predicted weakening due to clay

341 smearing for heterogeneous layers comprised of 30 and 40% clay fractions. The predicted weakening

342 is calculated using the arithmetic mean of the friction coefficients of the endmember quartz and clay

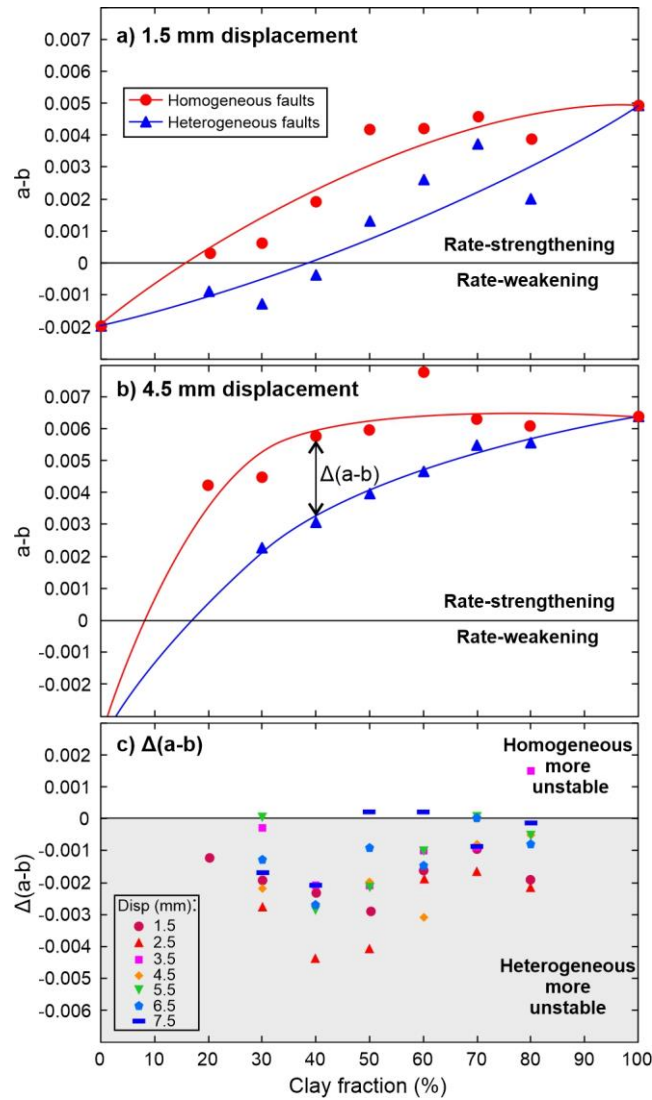
343 gouges and by assuming that the length of the clay patches increases by the amount of displacement on

344 the fault as clay is smeared along localized Y-shear planes. The observed weakening is considerably

345 greater than the predicted weakening. The labels (I), (II) and (III) correspond to the structural evolution

346 in **(b)**.

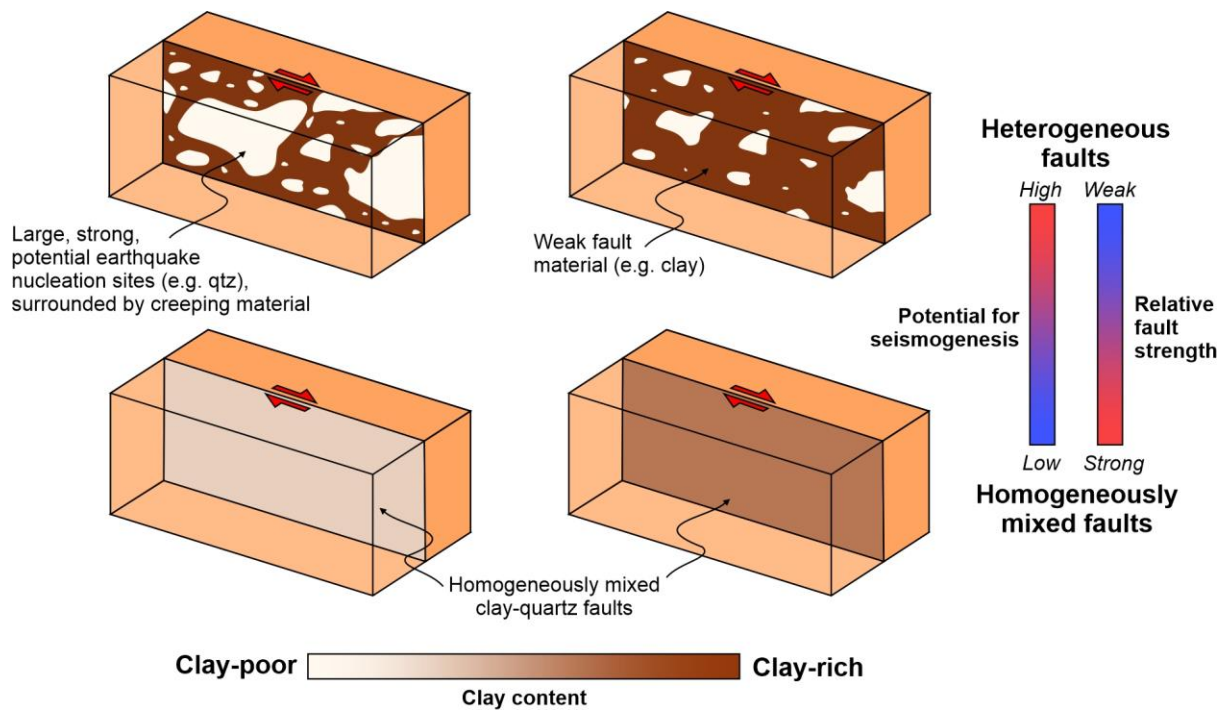
347



348

349 **Figure 3| Evolution of the stability-controlling rate-and-state friction parameter ($a - b$) as a**
 350 **function of clay content for the spatially heterogeneous and homogeneously mixed clay-quartz**
 351 **fault gouge layers. The ($a - b$) values are compared after a. 1.5 mm and b. 4.5 mm displacements, with**
 352 **the heterogeneous faults having consistently lower values than the homogeneous faults. c. The**
 353 **difference in ($a - b$) between the heterogeneous and homogeneous faults, $\Delta(a-b)$, is shown for all**
 354 **velocity steps across the entire displacement range, with the majority of values being negative,**
 355 **highlighting that the heterogeneous faults are less stable than their homogeneous counterparts. Note**
 356 **that, for displacements larger than 1.5 mm, the ($a - b$) values cannot be calculated for the homogeneous**
 357 **quartz fault (i.e., 0% clay fraction) or the heterogeneous fault with a 20% clay fraction, as stick-slip**
 358 **instabilities were triggered by the velocity steps.**

359



360

361 **Figure 4| Schematic fault model showing the effect of heterogeneity on fault strength and stability.**

362 For a given clay-quartz composition, the introduction of heterogeneity (i.e. the separation of clay and

363 quartz into patches) leads to a reduction in fault strength relative to a homogeneously equivalent fault

364 and also a decrease in stability, increasing the likelihood of seismogenesis on the fault.